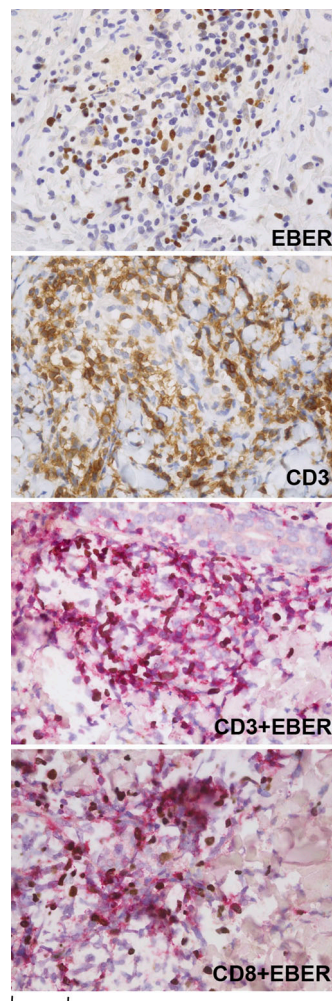Figure S1.   **Infiltrate of CD3+CD8+ T cells infected by EBV in hydroa vacciniforme–like lesions of the patient.** Skin biopsy of the hydroa vacciniforme–like lesions of the patient after staining with anti-CD3 (CD3) or an EBER probe or double staining with anti-CD3 or anti-CD8 antibody and EBER probe (CD3+EBER and CD8+EBER) showing skin infiltrate composed of CD3+ CD8+T lymphocytes that are infected by EBV. Magnification, ×400. Scale bar, 40 μm.
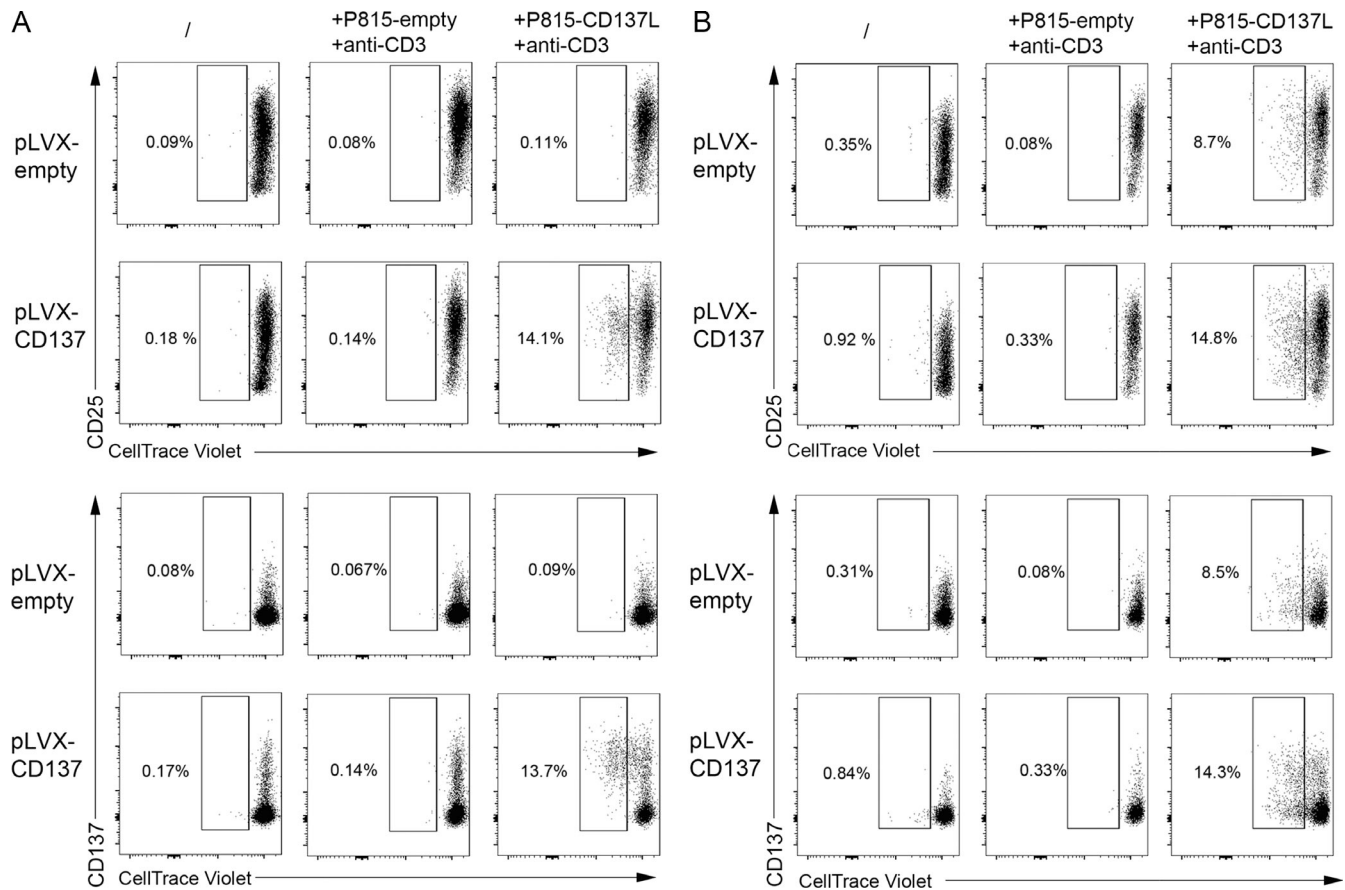
Figure S2. **Correction of CD137 expression in CD4⁺ CD137-deficient T cells restores their capacity to proliferate in response to CD137L-expressing cells. (A and B)** FACS dot-plots of proliferation assays of T cells from the sister (A) or a healthy control (B) in which CD137 was restored (pLVX-CD137) or not (pLVX empty) after incubation with the CellTrace Violet dye and cocultured or not (/) for 5 d with irradiated P815 cells expressing CD137L or not (P815-empty) in the presence anti-CD3 antibody. Cells were then stained with an anti-CD25 antibody (upper panels) as an activation marker or with an anti-CD137 antibody (lower panels) and analyzed by flow cytometry after gating on CD4⁺ T cells in A (for the sister) or on CD8⁺ T cells in B (for the control). Numbers represent the percentage of proliferating cells in corresponding gates. Experiments were done in duplicate with the same results. One replicate is shown.
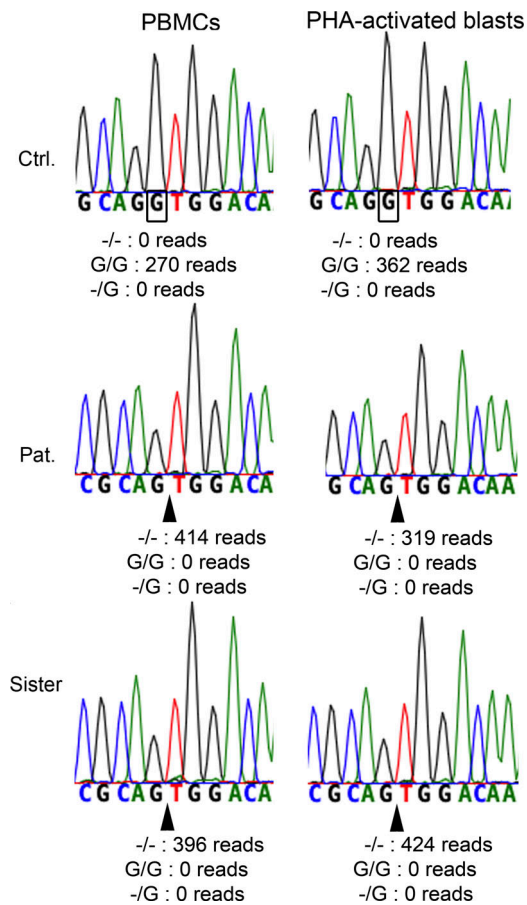
Figure S3. Sequencing of the mutation by Sanger or NGS does not reveal any reversion genetic event. DNA extracted from PBMCs or 72 h activated PHA-T cell blasts from a control (Ctrl.), the patient (Pat.), and his sister were sequenced for the mutation. DNA electropherograms from Sanger sequencing are shown with an arrow indicating the position of G, which is deleted in the patients and his sister, or by a box in the control electropherogram. DNA was also analyzed by NGS allowing the quantification of reads containing or not the deletion. The numbers of reads and the genotypes are shown under the arrows (for the patient and his sister) and under the boxes in the control with the G corresponding to the WT allele and the – to the G deleted allele.
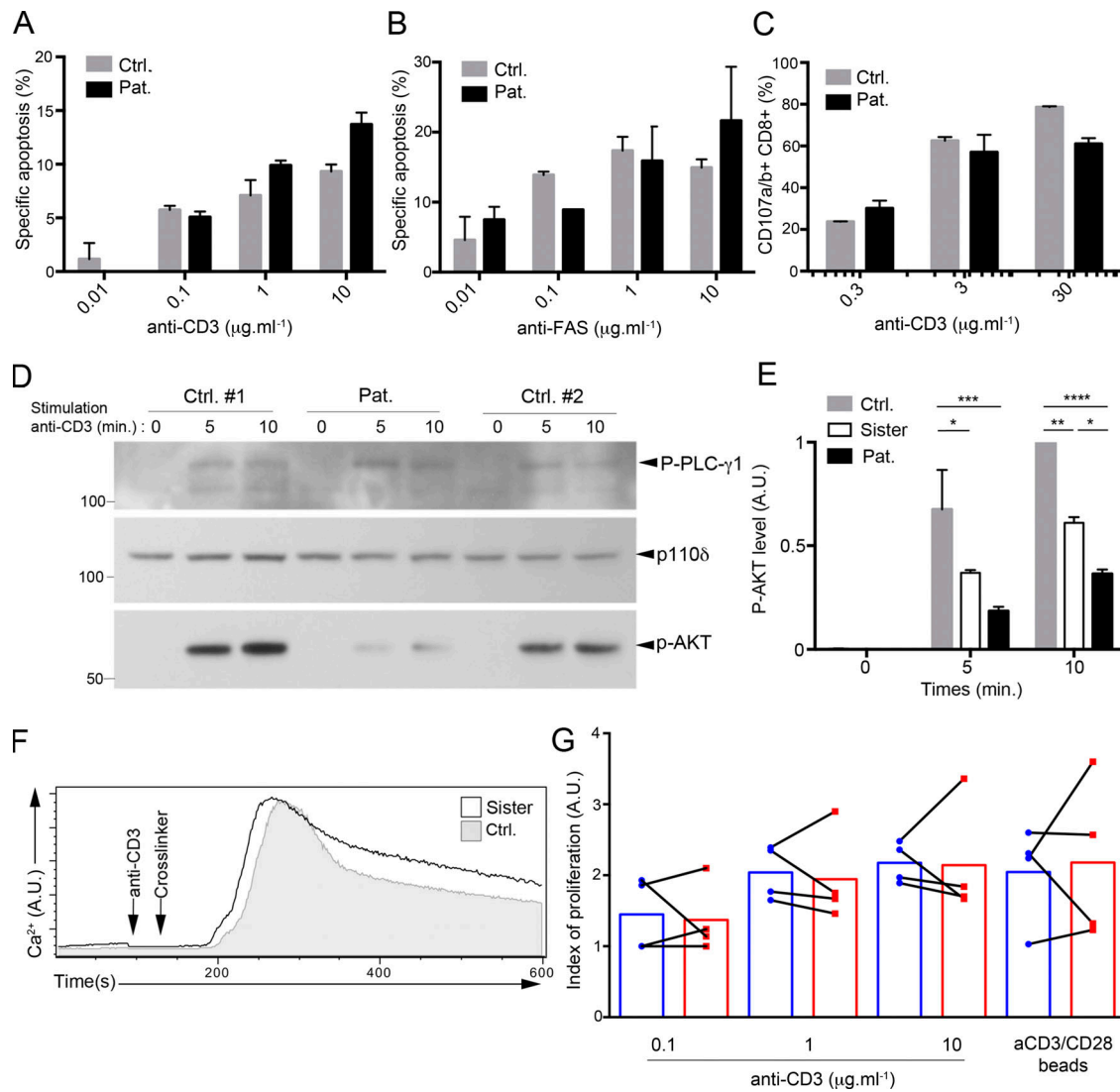
Figure S4. **Functional analyses of T cells from the patient and his sister. (A–C)** T cell blasts from the patient (Pat.) or a control (Ctrl.) were stimulated with different concentration of anti-CD3 antibody (A and C) or anti-FAS antibody (B). Apoptotic cells were determined after staining with Annexin V and viaprobe propidium iodide by flow cytometry. Results show the percentage of specific induced apoptosis calculated from dot-plots of FACS analysis after gating. **(C)** Degranulation was analyzed after 3 h of stimulation by staining with anti-CD107a/b and anti-CD8 antibody by flow cytometry. Results show the percentage of CD8$^+$CD107a/b$^+$ releasing cytotoxic granules calculated from dot-plots of FACS analysis after gating. **(D)** Immunoblots of phosphorylated PLC-γ1 (P-PLC-γ1), p110γ, and P-AKT in T cell blasts from the patient (Pat.) and two controls (Ctrl.#1 and Ctrl.#2) stimulated with anti-CD3 antibody for 0, 5, and 10 min. Molecular weight markers are shown on the left. **(E)** T cell blasts from the patient (Pat.), his sister, or a control (Ctrl.) were analyzed for P-AKT (Ser 473). Densitometry quantifications of immunoblots for phosphorylated AKT at Serine 473 of T cells stimulated for 0, 5, and 10 min. **(F and G)** T cell blasts from the sister or from a control (Ctrl.) were analyzed for intracellular Ca^{2+} levels (F) or proliferation (G). **(F)** Real-time flow cytometry after stimulation with anti-CD3 antibody and a cross-linker. **(G)** Proliferation of T cell blasts (Ctrl. in blue and sister in red) after incubation with the CellTrace Violet dye and stimulation or not (No stim.) with anti-CD3/CD28–coated beads (right) or coated anti-CD3 at different concentrations (left). Results show calculated proliferation indexes from FACS analysis of dye dilutions. One representative experiment of three independent experiments is shown in A–C and F. Data in E represent mean and SD from three independent experiments with mean and SD. Four independent experiments are shown in G. *, P < 0.05; **, P < 0.01; ***, P < 0.001; ****, P < 0.0001 (one-way ANOVA with post hoc Bonferroni t test).
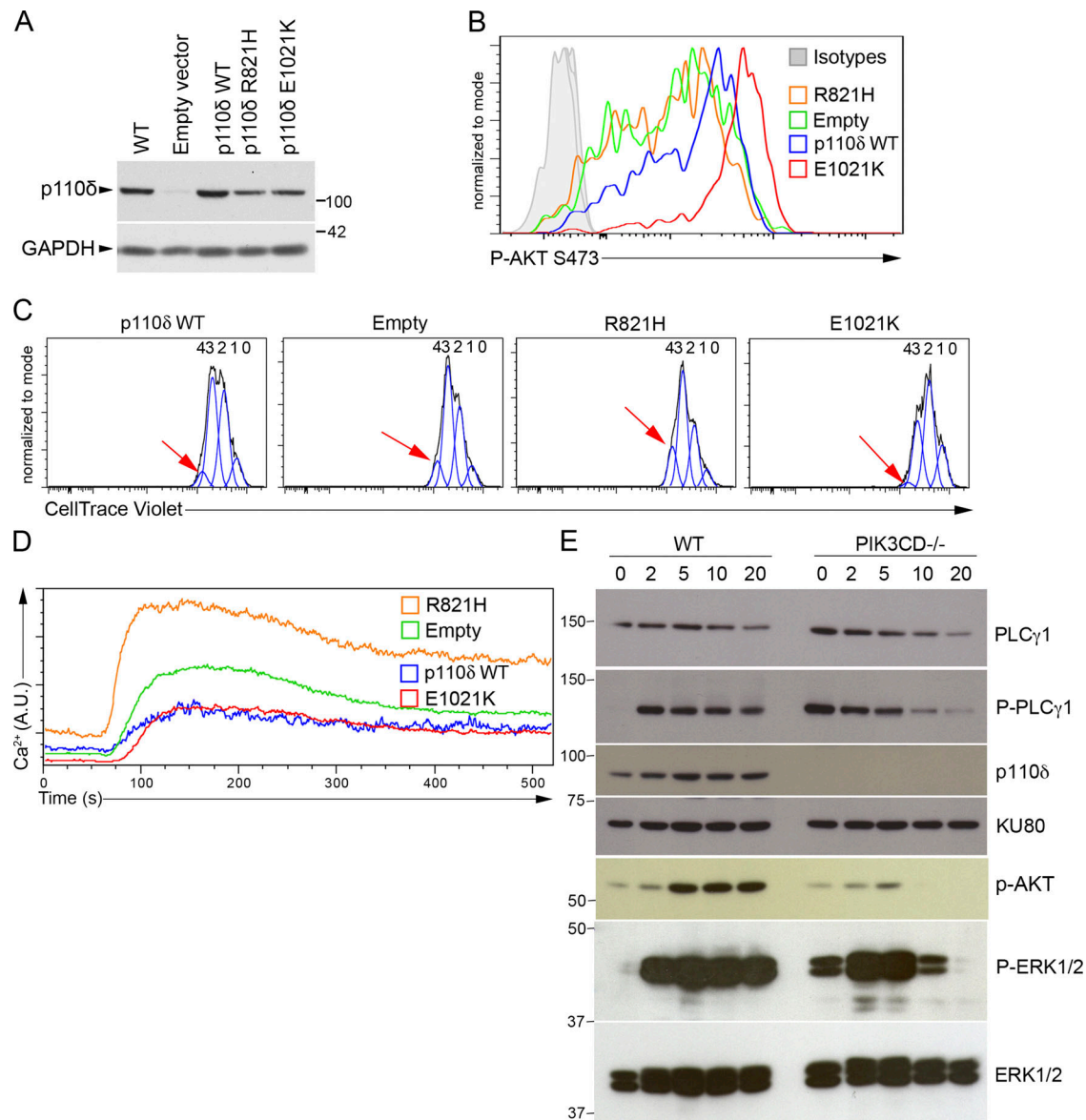
Figure S5. **Imbalanced PLCγ1–dependent signals in PIK3CD-deficient Jurkat T cells obtained by targeting *PIK3CD* exon 5 by CRISPR-Cas9. (A)** Immunoblot of p110δ expression in WT or exon 5–targeted PIK3CD-deficient (CRISPR exon 5 PIK3CD^−/−) Jurkat cells reconstituted with an empty vector (empty vector) or a vector coding for WT (p110γ WT), R821H, or E1021K p110δ. Immunoblot of GAPDH as loading control. Molecular weight markers are shown on the right. **(B)** FACS histograms of intracellular staining of the expression of phosphorylated AKT at serine 473 (P-AKT S473) in the different CRISPR exon 5 PIK3CD^−/− Jurkat cell lines shown in A. Isotype controls are in gray. **(C)** Histograms from plots of proliferation assays of the different CRISPR exon 4 PIK3CD^−/− Jurkat cell lines shown in A after incubation with the CellTrace Violet dye for 96 h and dye dilution analyzed by flow cytometry. Numbers in histograms ahead each peak correspond to the number of cell divisions. The red arrows indicate the peak of the fourth division in each histogram. **(D)** Intracellular Ca^{2+} levels analyzed by real time flow cytometry in the different CRISPR exon 5 PIK3CD^−/− Jurkat cell lines shown in A stimulated with anti-CD3 antibody. Data are representative of three (A) or two (B–D) independent experiments with two (C) or one (B and D) biological replicates per group in each. **(E)** Immunoblots of phosphorylated PLCγ1 (P- PLCγ1) and ERK1/2 (P-ERK1/2) in WT Jurkat (WT) or CRISPR exon 5 PIK3CD^−/− (PIK3CD^−/−) Jurkat stimulated with anti-CD3 antibody for 0, 1, 2, 5, 10, and 20 min. Total amounts of PLCγ1, PIK3CD (p110γ), KU80, and ERK1/2 are also shown. Molecular weight markers are shown on the left.